Sustainable Energy & Fuels

ROYAL SOCIETY OF CHEMISTRY

REVIEW

View Article Online
View Journal | View Issue

Cite this: *Sustainable Energy Fuels*, 2023, 7, 5608

Nanocomposite use in MFCs: a state of the art review

Karolina Kordek-Khalil, [a] Esra Altiok, [b] Anna Salvian,[cd] Anna Siekierka,[a] Rafael Torres-Mendieta, [e] Claudio Avignone-Rossa, [c] Andrea Pietrelli,[f] Siddharth Gadkari, [d] Ioannis A. Ieropoulos *[g] and Fatma Yalcinkaya *[e]

Microbial fuel cells (MFCs) have been gaining attention as a promising technology for sustainable energy production through the metabolic processes of microorganisms. The materials traditionally employed in this field have fallen short in facilitating efficient microbial-electron transfer and subsequent current generation, posing significant challenges for practical applications. To overcome this hurdle, the integration of nanomaterials into MFC components has emerged as a promising avenue, capitalizing on their unique physical and chemical properties to drive iterative advancements. In this review article, we explore the importance of nanomaterials in MFCs, highlighting their exceptional attributes such as high surface area-to-volume ratio, stability, durability, and selectivity. These advancements could hold the key to accelerating the recognition of MFCs as a powerful platform technology.

Received 28th July 2023
Accepted 13th October 2023

DOI: 10.1039/d3se00975k

rsc.li/sustainable-energy

1. Introduction

The ever-increasing demand for energy, the depletion of conventional energy sources, and the adverse effects of fossil fuels on the environment have led to the search for alternative energy sources. The vast majority of our global energy needs are met by fossil fuels, but they also release carbon, sulfur, and nitrogen oxide emissions, which are the main factors of climate change, the greenhouse effect, acid rain, and the hole in the ozone layer. Furthermore, as a result of contemporary ways of life, fossil fuel reserves are rapidly depleting whilst consumption of energy is sharply rising. Consequently, a critical fossil fuel shortage has been forecast for the future. This scenario highlights the necessity of using renewable energy sources, like solar, wind, biomass, and others, to provide electricity. In order to protect the environment and sustain economic growth, renewable energy sources must be better utilised. However, due to high capital and operating costs as well as poor conversion efficiencies, it is still challenging to render renewable energy-producing equipment commercially viable.[1–5] Considering the above, there is a substantial demand for environmentally friendly alternatives as sources of energy or fuel. These sources must meet specific sustainability requirements such as minimal carbon footprint,[6] affordability,[7] safety,[8] and the possibility of being employed in off-grid areas, particularly in developing countries, where access to electricity is crucial for social development and well-being.[9] While various options have been explored over the years, bioelectrochemical devices known as microbial fuel cells (MFCs) are gaining a lot of attention due to their ability to fulfill all the sustainability requirements.[10] Moreover, their unique advantage of harvesting electricity from organic compounds using electroactive microbes, opens up a new horizon in bioelectricity, while reducing organic waste.[11] In the MFCs, microbes, such as anodophilic cable bacteria, are used as catalysts to break down wastewater,[12] food waste,[13] or agricultural waste[14] into carbon dioxide,[15] hydrogen,[16] methane,[17] and electrons.[18–20] The catalytic oxidation of this organic matter occurs at the anodic half-cell connected to a cathodic counterpart and separated by a cation or anion exchange membrane (CEM or AEM). The released electrons are transferred to the anode electrode, and move towards the cathode through an external circuit. At the same time, cations such as protons move from the anodic chamber to the cathode through the membrane and combine with (*e.g.*) oxygen from air and those incoming electrons to complete the reactions and generate current. Thus, MFCs generate electricity and biofuels from ubiquitous materials while helping to reduce the amount

[a]*Department of Process Engineering and Technology of Polymer and Carbon Materials, Faculty of Chemistry, Wrocław University of Science and Technology, Wrocław, Poland*
[b]*Institute of Mechatronics and Computer Engineering, Faculty of Mechatronics, Informatics and Interdisciplinary Studies, Technical University of Liberec, Liberec, Czech Republic*
[c]*Department of Microbial Sciences, University of Surrey, Guildford GU2 7XH, UK*
[d]*School of Chemistry and Chemical Engineering, University of Surrey, Guildford GU2 7XH, UK*
[e]*Institute for Nanomaterials, Advanced Technologies and Innovation, Technical University of Liberec, Studentská 1402/2, 461 17 Liberec, Czech Republic. E-mail: fatma.yalcinkaya@tul.cz*
[f]*Univ Lyon, Université Claude Bernard Lyon 1, INSA LYON, Ecole Centrale Lyon, CNRS, UMR 5005 Ampere, Villeurbanne, F69622, France*
[g]*Department of Civil, Maritime & Environmental Engineering, University of Southampton, Bolderwood Innovation Campus, Burgess Road, Southampton, SO16 7QF, UK. E-mail: I.Ieropoulos@soton.ac.uk*

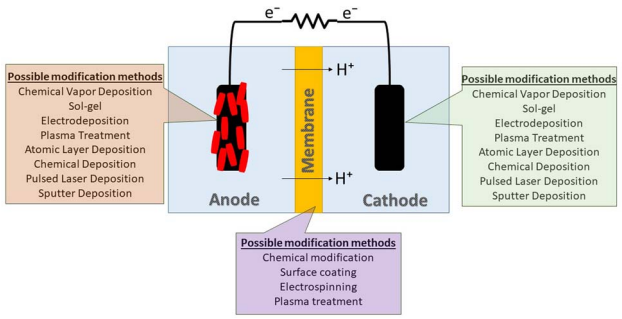

Fig. 1 MFC components and possible modification techniques of these components.

of organic waste that would otherwise pollute the environment, making them highly sustainable.[21] Although such benefits place MFCs as a potential green alternative to traditional fossil fuel-based energy sources, they still face challenges that limit their practical applications, due to the suboptimal components used.[22] Therefore, optimising MFC components is critical to enhancing their performance and therefore feasibility.[23]

In response to such a need, the scientific community recently focused on improving the MFC components using nanomaterials, whose unique physical and chemical properties have profoundly improved their performance.[24–30] Besides providing structural resistance[31] and improving the electron transfer rate through the electrode[32] and membrane proton transfer selectivity,[33] their exceptional volume-to-surface ratio can control the microbial adherence and retention on the electrode surface, thereby optimizing the bacterial anode electron transfer.[34] For the cathodic half-cell, nano-modification can provide sufficient porosity to facilitate oxygen diffusion through its surface, enabling higher rates of oxygen reduction reaction (ORR) and consequently, current generation.[35] Fig. 1 presents a depiction of the components of MFCs and the diverse techniques employed for modifying them with nanomaterials. Xiao *et al.*[36] for example, improved electricity generation in MFCs through a straightforward modification technique that involved applying reduced graphene oxide (rGO) and a Nafion coating to carbon cloth. Fig. 2 illustrates a straightforward modification technique applied to both the anode and cathode electrodes of an MFC unit. Nanomaterials such as those based on carbon, can independently reinforce each part, offering greater durability and stability, thus improving material integrity.[37] This can extend the MFC longevity and reduce operational costs.[38]

MFCs have the potential to be an important contender as a platform technology for energy generation, waste treatment, resource recovery and environmental remediation, and are therefore becoming a global research priority.[39,40] This review discusses the state-of-the-art of nanomaterials in MFC components. We highlight the advantages and limitations of their usage and provide an outlook for future research and development in this area, which represents a growing field with the potential to create value from waste, thereby benefiting our society by helping us shift to a more circular and sustainable economy.

1.1. Fundamentals of microbial fuel cells

Unlike chemical fuel cells that use chemical catalysts, electrochemically active microorganisms are instead used as biocatalysts in MFCs.[41] Electron-donating microorganisms are called anodophilic while electron accepting organisms are called electrotrophs.[41–43] Microorganisms use organic matter as a source, oxidise the organic matter by metabolic processes and generate electricity by following the reaction[18,19,44–46] as shown for a single-chamber air–cathode microbial fuel cell:

$$\text{Anode reaction: } C_2H_4O_2 + 2H_2O \rightarrow 2CO_2 + 8H^+ + 8e^-$$

$$\text{Cathode reaction: } 2O_2 + 8H^+ + 8e^- \rightarrow 4H_2O$$

$$\text{Overall reaction: } C_2H_4O_2 + 2O_2 \rightarrow 2H_2O + 2CO_2$$

As mentioned above, the oxidation/degradation-reduction potential in the reactor yields electrons that flow from the

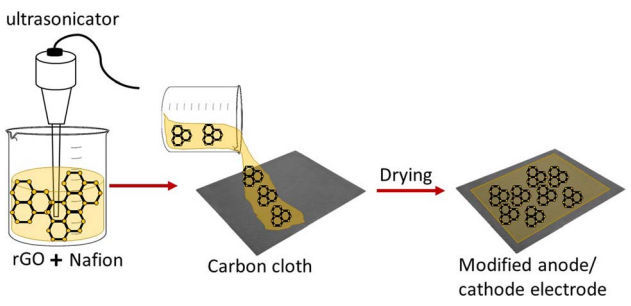

Fig. 2 A simple modification of the anode and cathode electrode of an MFC unit.

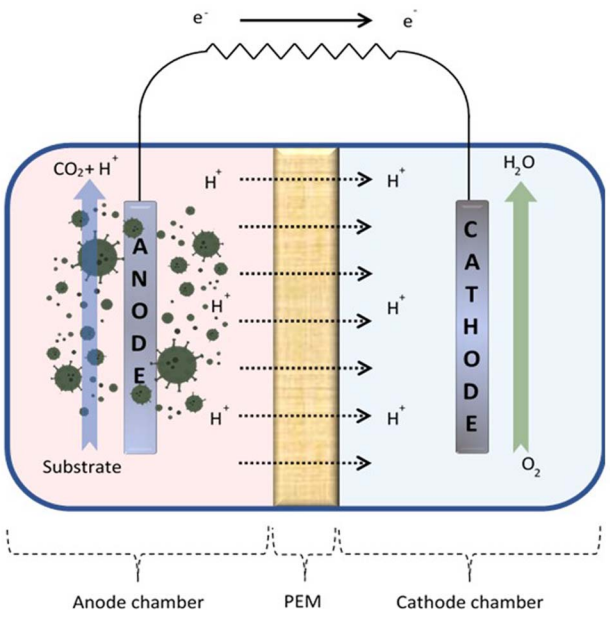

Fig. 3 Simple illustration of an MFC assembly.

anode to the cathode compartment in which the final electron acceptor—*e.g.*, oxygen—is available. In a typical MFC unit, there are anode and cathode chambers that are separated by a separator membrane (proton/cation exchange membrane)[1,47,48] as shown in Fig. 3.

The image shows that the organic matter is broken down, *via* microbial anaerobic digestion, releasing electrons and cations (here shown as protons). Electrons move through the external circuit, whereas protons diffuse through the membrane, and through the continuous reaction with oxygen at the cathode, the gradient is maintained for more H^+ ions and electrons to flow. In an MFC, electricity is produced only when the total process is thermodynamically advantageous.[3]

As with every physical system MFCs are subject to internal losses, which can be classified as activation, ohmic and mass transfer losses.[49] Parameters, such as temperature, pH, substrate type, microorganism type, electrode material, proton exchange membrane characteristics and reactor design, all play a role in the performance of MFCs. In order to optimise energy production in MFCs, it is crucial to carefully examine these parameters while constructing and operating MFCs.[1,3,41,50–55]

MFCs generate energy from a variety of refined and unrefined substrates, including domestic and industrial wastewater, molasses, dairy, oil refineries, textile dye industry, tannery, breweries, food industry *e.g.*, chocolate making, paper industry, *etc.*[1,56,57] MFCs may be utilized for a variety of applications, such as biosensors, environmental monitoring,[58–61] onsite power production in remote regions and removing contaminants from groundwater in addition to wastewater treatment and energy production.[62–65]

2. Nanomaterials for MFC anode electrodes

2.1. Ideal properties of an anode material

MFC performance, accessibility, and scalability are greatly influenced by the electrode design. Several features of the anode influence the performance of MFCs, namely electrical conductivity, surface area and porosity, biocompatibility with electroactive bacteria (EB), mechanical strength, and chemical stability.[66–69] Moreover, the availability and price of the raw material should be taken into consideration when selecting an appropriate electrode, as this might have a major impact on the sustainable implementation of large scale MFCs.[70] For this reason, the selection of suitable anode materials, which can promote growth of EB and extracellular electron transfer (EET), is a common focus of MFC performance improvements.[71–73]

Nanomaterials have gained increasing attention in the electronic, MFC and electrochemical fields over the last 15 years due to their outstanding properties, most notably a very high surface area.[27] Nanomaterials are substances with at least one dimension smaller than 100 nm, while "nanocomposites" refers to multiphase materials with at least one phase having a dimension smaller than 100 nm.[74] Some nanomaterials, such as reduced graphene oxide (rGO) and carbon nanotubes (CNTs), have been incorporated into other materials, such as polymers and metals, to enhance their properties and obtain nanocomposites with good potential for MFC electrode applications. These additional properties include excellent porosity and surface area, conductivity, thermal stability, mechanical strength, and resistance to corrosion. In this section, we list the most recently created nanomaterials and nanocomposites that have been successfully used in MFCs as electrode materials.[75,76]

Table 1 shows more details about how each of the aforementioned factors affects the performance of the anode, demonstrating the crucial role of nanomaterials in enhancing MFC performance.

In the last two decades, researchers have focused on developing innovative electrode materials and anode surface modification methods to enhance the performance of MFCs. Nanomaterials, including metals, conductive polymers, nanotubes, nanowires, nanoparticles, and quantum dots, have become increasingly popular.[26,40,66,77,78]

2.2. Classification of nanomaterials for MFC anode electrodes

Many different functional nanomaterials have been tested in MFCs and exhibited unique advantages compared to their common macro-sized equivalents.[79] These nanomaterials can be classified into different groups: carbonaceous nanomaterials, metals and metal oxides, and conductive polymers, which can also be combined to form composites with enhanced properties.[26] Table 2 summarises the performance of MFCs equipped with different nanomaterial-containing anodes.

2.2.1. Carbon-based nanoparticles and nanocomposites. Due to their low production cost, low inherent toxicity, and versatile surface functionalization, carbon-based nanoparticles are among the most extensively researched materials in the field of nanotechnology.[27,80] There are different types of carbon-based nanoparticles, namely carbon nanotubes (CNTs), graphene, and carbon nanoparticles (CNPs).

2.2.1.1 Carbon nanotubes. CNTs have been selected in several studies for their high surface area, mechanical strength, and ability to improve EET from the biofilm to the electrode.[81] They are made of graphite sheets and have cylinder-shaped tubular structures with one or more walls, having dimensions between single units and tens of nanometers.[82] The high surface area of CNTs is crucial for healthy biofilm growth and good electrical contact to ensure adequate electron exchange among bacteria and the anode.[83] In fact, it has been demonstrated that with common carbonaceous electrodes, after a few months of operation, the biofilm on the anode surface becomes too thick, limiting the current production due to the number of dead or non-electroactive cells accumulating inside the biofilm matrix and reducing the diffusion of the organic substrates in the anolyte.[69,84,85] In a recent study, CNTs altered the shape of the anode surface, favouring the growth of EB and extracellular flagellated microorganisms (such as *Shewanella* spp.), which resulted in a more efficient EET.[86] Furthermore, MFCs with CNTs on a stainless steel (SS) mesh anode decrease ohmic losses and increase power generation (from 72 mW m^{-2} for bare SS to 327 mW m^{-2}) thanks to their electrocatalytic activity.[87] One

Table 1 Factors affecting anode performance in MFCs

Anode feature	How it affects MFC performance	Ref.
Electrical conductivity	High conductivity of the electrode ensures that electrons can move through the material with minimal ohmic resistance, avoiding power losses	92
Surface area and porosity	Material porosity and surface area affect the distribution and thickness of the catalytic biofilm at the anode, and consequently the overall performance and stability of MFCs. Higher surface area increases the likelihood of greater contact between the electrode and the biofilm, which results in increased EET. Additionally, high porosity and pore sizes in the order of hundreds of micrometres are essential for delaying biofilm overgrowth, which leads to anode clogging, thus optimising the mass transfer of the substrates to the cells	84, 85 and 93
Biocompatibility with EB	A hydrophobic and positively charged electrode surface attracta the EB, which have a negatively charged membrane, speeding up the transfer of electrons while also promoting bacterial adhesion	94
Material strength and resistance to corrosion	Resistance to mechanical deformation and high chemical stability ensure longer operational stability of the anode	95

strategy is to dope CNTs with positively charged molecules, such as polyaniline (PANI) or polyethyleneimine (PEI). Due to the strong interactions of PANI with CNTs and stable bonding, the use of a PANI/CNT nanocomposite provides environmental stability and good electrical conductivity.[88] PANI and PEI attract the negatively charged membrane of EB, favouring better adhesion of the catalytic biofilm and a more efficient EET.[89,90] Qiao *et al.* found that the mass ratio between CNTs and PANI has an influence on the performance of MFCs, with 20% CNTs being the best concentration to enhance the surface area and EET.[91]

2.2.1.2 Graphene. In the late 90s, it was demonstrated that materials containing electron acceptors, such as Fe(III), can increase the growth of metal reducing bacteria.[96] Tests using an Fe-doped graphene anode showed increased power generation and water remediation using MFC technology.[96] In these studies, Fe-doped graphene promoted the development of a uniform EB biofilm, leading to higher power densities (3220 mW m^{-2}).[97] Moreover, heteroatoms can be chemically incorporated into graphene to improve its conductivity. Nitrogen was successfully doped onto the surface of graphene sheets,[98] demonstrating that P-type doping facilitates positive charges to delocalize in the anode and that porous network architectures improved the adhesion of EB and encouraged direct electron transfer.[98]

Different species of graphene, graphene oxide (GO), reduced graphene oxide (rGO), and graphene particles have been extensively employed in MFCs during the last few years.[92] The main advantage of graphene nanoparticles is their superior electron-shuttling properties compared to ordinary graphite and CNTs, which results in faster EET. Graphene transfers current more efficiently than graphite and CNTs. This is due to its high crystal quality, allowing electrons to travel through the material without scattering. Compared to all other carbon materials, graphene permits higher electron mobility, which suggests that graphene-based electrodes will theoretically be considerably more efficient.[99] Moreover, the presence of oxygen-containing functional groups makes the graphene surface hydrophilic, which favours electroactive biofilm formation.[100]

Graphene nanoparticles can be combined with other materials to create novel nanocomposites with unique properties, which can further improve the performance of the MFC anode. For instance, GO nanoparticles, which consist of graphene with a higher number of oxygen-containing functional groups, have also been combined with normal graphene to enhance the hydrophilicity and biocompatibility of the anode in MFCs, obtaining a power density 1.51 times higher than that of bare graphite anodes.[101] The main drawback of using GO is the high resistivity of the material. To increase the conductivity, rGO nanoparticles have also been widely used in MFC anodes, showing better performance than GO.[102] rGO and polyacrylamide (PAM) were combined utilising polymerization procedures (graphene/rGO/PAM), producing maximum power densities of 782 mW m^{-2}.

2.2.1.3 Other carbon nanoparticles. Carbon nanoparticles (CNPs) are categorised as a unique form of carbonaceous spherical nanomaterials with diameters below 10 nm. The primary benefit of CNPs is that they can be made from waste materials *e.g.*, candle soot rendering MFC anodes both economically affordable and effective. The study shows that EET at the electrode surface was facilitated by the graphitic CNPs, reaching power densities of up to 1650 mW m^{-2}.[103] Another advantage of CNPs is that they also enable the immobilisation of microorganisms around the carbon structures to control the cell density and increase the efficiency of EET of the catalytic biofilm.[104]

CNPs can also be doped with heteroatoms to improve MFC performance. A carbon cloth-based anode coated with porous carbon nanoparticles obtained from tannic acid (a plant polyphenol) and doped with heteroatoms (N, P, S, and Co) produced a power density that was 1.82 times greater than that of regular carbon cloth. The innovative anode material also significantly

Table 2 Performance of MFCs equipped with different NP-containing anodes

Anode			Fold change of power output improvement[a]	Type of inoculum	Power output (mW m^{-2})	Ref.
Support material	Functionalisation	Cathode				
Carbon-based nanomaterials						
SS	CNT	Ni foam air cathode	3.63	Mixed inoculum	327	87
SS	CNT/PANI	SS mesh in buffer saline solution	1.71	Mixed inoculum	48	88
N-CNT	S	Graphite rod in potassium ferricyanide	1.71	*Shewanella oneidensis* MR1	712[b]	89
Graphene	GO	AC/PTFE air cathode	1.51	Mixed inoculum	1100	101
Carbon paper	PDDA/rGO	Carbon paper in potassium ferricyanide	2.51	*Escherichia coli*	5029	102
Graphene	PAM/rGO	Carbon cloth/Pt air cathode	2.17	Mixed inoculum	782	140
Carbon cloth	FeS_2/rGO	Graphite fiber brush in potassium ferricyanide	1.42	Mixed inoculum	3220	97
N-doped graphene nanosheet	—	Carbon cloth in potassium ferricyanide	n.s[d]	*E. coli*	1008	98
SS	Candle soot derived CNP	SS disk in potassium ferricyanide	n.s[d]	*E. coli*	1650	103
Carbon cloth	Heteroatom-doped CNP	Carbon cloth/activated carbon air cathode	1.82	Mixed inoculum	1720	105
Carbon cloth	Nitrogen-doped CNP	Carbon brush in potassium ferricyanide	3.50	*Shewanella putrefaciens*	2102	106
Metal-based nanomaterials						
Carbon cloth	Au NP/CNT	Graphite felt in potassium ferricyanide	1.56	*S. oneidensis* MR1	178	110
Carbon cloth	Pd NP	Carbon paper/Pt air cathode	1.21	Mixed inoculum	824	111
Carbon nanofibers	Ni NP	Carbon nanofibers/Ni NP	6.36[c]	*E. coli*	1145	112
Graphite	Fe carbon dots	SS/Pt–C air cathode	1.54	*S. putrefaciens*	440	114
Loofah sponge	TiO_2 NP	PTFE/carbon cloth/Pt–C air cathode	1.63	Mixed inoculum	2590	115
Carbon felt	$MnCo_2O_4$	Carbon felt in potassium ferricyanide	3.80	Mixed culture	945	116
Polymer-based nanomaterials						
Carbon cloth	PANI	Carbon cloth/Pt air cathode	2.66	Mixed culture	5160	121
Carbon felt	PANI	n.s[d]	1.35	Mixed culture	27	122
Carbon cloth	PANI nanoflower	Carbon felt in potassium ferricyanide	6.50	*S. oneidensis* MR1	389	124
PPy nanotube membrane	—	n.s[d]	6.65	*S. oneidensis* MR1	612	126
SS	PPy nanotube/ chitosan/NiO	PTFE/SS/Pt–C air cathode	4.90	Mixed inoculum	755	129
Carbon paper	PEDOT nanoparticles	Carbon paper in potassium ferricyanide	1.43	*Shewanella loihica*	140	130
SS	PEDOT/graphene/Ni NP	Graphite rods	2.90[b]	*E. coli*	3200[b]	131
Biochar	PEDOT/$NiFe_2O_4$	Biochar in potassium ferricyanide	2.36	Mixed inoculum	1200	132

[a] Fold change of power output improvement compared to the electrodes containing no NPs within the same study. [b] Re-calculated to obtain comparable units of measurement. [c] Value estimated from figures. [d] n.s.: non specified.

improved the EET and cell growth of the EB in the biofilm.[105] Similarly, the EET of *Shewanella putrefaciens* considerably increases when using nitrogen-doped CNPs as an anode coating for carbon cloth, generating a power density 3.5 times higher than that of a regular carbon cloth anode. This is mainly due to the enhancement of the anodic absorption of flavins, a soluble electron mediator produced by *S. putrefaciens*.[106]

2.2.2. Metal-based nanocomposites. In MFCs, pure metals are typically employed as the supporting material for anode electrodes for their high conductivity and mechanical strength.[107,108] Despite the tendency of metals to corrode, several studies have shown that adding metal or metal oxide nanoparticles to an anode supporting structure made of carbon does not pose this issue, improving the electrochemical performance, and having a positive impact on the microbial population of the catalytic biofilm.[109–111] Both pure metal and metal oxide nanoparticles have been used to improve anode materials for MFC applications.

2.2.2.1 Pure metal nanoparticles. Among the pure metals, gold is known to have poor biocompatibility, but when coupled with carbon paper it accelerated the growth and EET of *Shewanella oneidensis* MR-1, resulting in a 47% increase in power density.[109] Gold nanoparticles, together with CNTs, also enhanced the performance of MFCs inoculated with a mixed community, resulting in a rise in the number of EB, especially *Negativicutes*.[110] Carbon electrodes decorated with Pd nanoparticles showed a better maximum power density (824 ± 36 mW m^{-2}) compared to a nonwoven carbon cloth electrode (680 ± 28 mW m^{-2}).[111] A similar output was shown when Ni has been dispersed on carbon nanofibers to fabricate the anode of MFCs. Ni facilitates the mediated electron transfer of an *Escherichia coli* biofilm, resulting in a low charge transfer resistance and high power density (1145 mW m^{-2}).[112]

2.2.2.2 Metal oxide nanoparticles. Although pure metals have an outstanding electrical conductivity, metal oxides are generally preferred for their better biocompatibility and rough surface.[113] Carbon quantum dots coated with iron (II,III) oxide (Fe_3O_4) were coated on graphite anodes, generating a power output of 440.01 mW m^{-2}, 1.54 times greater than that of MFCs employing bare graphite sheet anodes. This is mainly due to the increased surface area and hydrophilicity of the electrode surface, which generally boost the growth of an electroactive biofilm.[114] Titanium dioxide nanotubes have also gained attention recently, for similar reasons as above. For instance, a graphite anode with TiO_2 nanoparticles and egg white protein derivatives was reported to produce a power density of 2590 ± 120 mW m^{-2} (210% higher than that of pristine graphite anodes). Multiple reasons, including a higher density of microorganisms adhering to the anode surface, a lower charge transfer resistance, and a larger contact surface with bacteria, could be responsible for this remarkable increase in power density.[115] Analogously, $MnCo_2O_4$ nanoparticles as a coating for a carbon felt anode has been shown to have good bioelectrochemical activity, reaching a maximum power density of 945 mW m^{-2}, 3.8 times higher than the one generated by the uncoated carbon anode control.[116]

2.2.3. Polymer-based nanocomposites. Conducting polymer nanocomposites are a promising material for a variety of applications due to their better electrical properties, low toxicity, availability, and low cost.[117]

2.2.3.1 Polyaniline (PANI). Polyaniline (PANI), a nitrogen-containing polymer, has been extensively used for electrochemical energy production and storage due to its simple synthesis, excellent environmental stability, cheap manufacturing cost, and high nitrogen content.[118–120] The positive charges given by the nitrogen atoms present on the surface of PANI increase the adhesion of the electroactive biofilm and enhance EET.[121] For this reason, the physical structure of PANI has been modified to optimise the surface area and pore size, providing an anode with optimal features and increased MFC performance.[122,123] It has been shown that the concentration of aniline for the polymerization of PANI on carbon cloth has an influence on the final physical structure of the coating. Nanoflower morphology gave the best maximum power density output (388.6 mW m^{-2}), 6.5 times more than that of a pristine carbon cloth anode.[124]

2.2.3.2 Polypyrrole (PPy) nanotubes. Polypyrrole (PPy) nanotubes have also been used due to good biocompatibility, simple synthesis, and low cost.[125] A PPy nanotube membrane was fabricated through a self-degraded template method, which involves an easy mix of reagents and drying steps and was used as an MFC anode, showing a 2.5-fold increase in current density compared to a carbon paper anode due to a higher specific surface area, improved EET, and higher conductivity of PPy.[126] Nonetheless, previously reported literature shows that PPy nanostructures exhibit poor stability and undergo reduction.[127,128] Therefore, to enhance its stability, coating of an SS anode with a composite made of PPy with a highly porous, biocompatible, good film forming material such as chitosan and NiO showed a reduction in the charge transfer resistance of the anode by 4.9 times compared to an uncoated SS anode.[129]

2.2.3.3 Poly(3,4-ethylenedioxythiophene) (PEDOT). Poly(3,4-ethylenedioxythiophene) (PEDOT) has also been investigated previously.[130] In a recent study, a low-cost and eco-friendly anode material produced by electropolymerization of PEDOT on rGO/Ni nanoparticles generated a high power density of 3200 mW m^{-2}.[131] Similarly, biochar supporting structures coated with $NiFe_2O_4$ nanorod/poly(3,4-ethylenedioxythiophene) (PEDOT) were used as a cheap and effective binder-free anode in MFCs, providing a power density of 1200 ± 60 mW m^{-2}.[132]

3. Nanomaterials for MFC cathode electrodes

3.1. Ideal properties of a cathode material

Conventional MFCs comprise an anode and a cathode and may or may not include an ion-exchange membrane. Therefore, the type and functionality of electrodes are critical for effective power production and despite the focus on the anode electrode, the cathode material has an equal impact on power production and longevity, which often is the limiting factor.[133,134]

Both electrode materials should be characterised by their high-performance, functionality, relatively low-cost and availability. An ideal cathode material should have high electrical conductivity, a high surface area to volume (SA/V) ratio, and chemical stability.[135] It should also be noncorrosive and fouling/scaling resistant. In the cathode, oxygen, as a gas, reacts and is reduced. Thus, the formed protons (H^+) diffuse in the electrolyte while electrons (e^-) are transported *via* a metallic wire from

the anode. Some part of the energy output of MFCs is consumed in the oxygen reduction reaction (ORR) activation. The reduction of the generated voltage caused by this phenomenon is often expressed as the ORR overpotential, which can be reduced by applying the appropriate electrocatalytic materials.[136] In the MFC setup, the ORR can follow the preferable 4-electron mechanism that leads to complete reduction of O_2 to H_2O or the 2-electron mechanism that results in the formation of H_2O_2.[137] The latter product can act as a harmful aggressive oxidant.[138,139] The appropriate choice of an electrocatalyst can increase the selectivity of the ORR toward the desired product. This section discusses various types of cathode materials in MFCs.

3.2. Classification of nanomaterials for MFC cathode electrodes

3.2.1. Carbon-based metal-free materials. Even though platinum is regarded as the most active ORR electrocatalyst, its scarcity and prohibitive cost have driven the search for alternative cathodic materials prepared from earth-abundant elements. As the price of activated carbon (AC) per kilogram is approximately 50 000× lower than that of platinum, this high surface area material has been widely studied as an essential constituent of cathode materials for MFCs.[141]

Carbon materials composed of only carbon and oxygen often have limited ORR activities due to the chemical inertness of graphene layers. Therefore, introducing heteroatoms (N, S, and P) to the carbon network is a practical approach to boost the cathode performance. This strategy affects the conjunction of carbon electrons with the lone-pair electrons from heteroatom dopants and their activation in electrochemical reduction.[133] In recent years, practical cathodes were obtained by forming nitrogen-doped carbon aerogels (CAs), possessing the advantage of hierarchical porosity. While micropores act as ORR active sites in such materials, meso- and macropores function as oxygen transport channels.[142]

Highly nitrogen-doped CAs were prepared from PANI obtained by emulsion polymerisation, hydrothermal treatment, and pyrolysis at different temperatures.[134] The best-performing material obtained by pyrolysis at 800 °C has a high surface nitrogen concentration of 25 at%. An MFC cathode with a low catalyst loading of 2 mg cm^{-2} (on carbon cloth) shows a maximum power density of 1048 mW m^{-2}. The authors attribute its high activity to high concentrations of pyridinic and graphitic nitrogen. Among the forms of nitrogen in carbon materials, pyridinic nitrogen induces the highest charge density on neighbouring carbon atoms, creating more electrocatalytically active spots.[143]

In another line of work, nitrogen-doped CA was formed by a hydrothermal process followed by freeze-drying.[144] The study focused on the effect of subsequent product activation using KOH at various CA : KOH ratios. This treatment strongly influenced not only the surface area of the material but also the nitrogen and oxygen functional group concentration and distribution. The MFC cathode with the highest performance was obtained by activation with the lowest CA : KOH ratio. Despite a relatively low surface nitrogen concentration (<1 at%), it delivered a maximum power density of 967 mW m^{-2} with an activated CA loading of 20 mg cm^{-2}. The ORR performance showed direct proportionality with pyridinic N content.

Other ideas for improving the cathode performance include changing its configuration in the MFC setup. Chen *et al.*[133] proposed substitution of a traditional 2D air–cathode by a rotating 3D air–cathode, which increases the number of available catalytic sites and avoids performance limitations due to low O_2 and OH-mass transfer rates. The cathode was formed by oxidative polymerisation of aniline on a pre-oxidised graphite brush (GB), which resulted in the formation of PANI, further pyrolysed with phytic acid. As a result, nanostructured N, P-doped carbon was formed on the GB. The electrode rotated at 20 rpm delivered a power density of 879 mW m^{-2}, double that of the electrode used in a static mode. A low revolution rate was chosen to simulate the desired operating conditions in which the rotation of the cathode could be driven by wastewater flow without external energy consumption.

Furthermore, using carbon–carbon composites can effectively boost the cathode performance in MFCs. For example, in a study by Koo *et al.*[141] in a cathode composed of AC and carbon black (CB), the latter component was partially replaced by reduced graphene oxide (rGO) at different CB : rGO weight ratios. Both CB and rGO are the electrode components assuring high electrical conductivity of the composite, with the conductivity of rGO *c.a.* 3 times higher than that of CB. As the study has shown, the highest maximum power output of 2642 mW m^{-2} was exhibited by the cathode in which the CB : rGO mass ratio was 1 : 1. At elevated rGO concentrations, the power performance was lower, presumably because the carbon nanocomposite film formed, at the stainless steel current collector which had increased thickness that resulted in the formation of surface cracks.

3.2.2. Metal-based materials and their composites. Researchers are directed towards developing platinum group metal (PGM)-free alternative electrode materials. First–row transition metals are quite often investigated, especially: Fe, Co, Ni, Mn and Cu.

Many electrocatalysts include transition metal oxides and hydroxides with nanosized morphologies. For instance, nanoparticles composed of metallic nickel and nickel oxides were plated on carbon felt by electrophoretic deposition to form the MFC cathode directly.[145] The cathode in the MFC setup delivered a maximum power of 1630.7 mW m^{-2}. In other examples, MnO_2 nanorods were coated on carbon cloth by electrodeposition. Due to the limited conductivity of the material, the nanorods were partially reduced by calcination at 250 °C in a H_2 atmosphere to create oxygen vacancies that act as shallow electron donors boosting electric conductivity and creating more electrocatalytically active sites. Thus, in MFCs, non-stoichiometric defective manganese oxide nanorods showed a maximum power density of 1639 mW m^{-2}.

As already mentioned, combining two or more metals in one electrocatalytic material is an effective strategy to boost the activity of a nanomaterial. Nanocrystalline mixed CoO–NiO oxide was obtained from cobalt and nickel chlorides using a leaf extract as a chelating agent.[146] The maximum power density

achieved by the cathode prepared by deposition of this material on carbon cloth was 703 mW m^{-2}, significantly higher than that of monometallic CoO (616 mW m^{-2}) and NiO (545 mW m^{-2}) analogues. Also, in another study, to increase the conductivity of MnO_2 nanorods, Co_3O_4 nanoparticles were deposited on their surface, creating a two-phase nanocomposite.[147] This operation resulted in an upsurge in the maximum power density of the MFC to 475 mW m^{-2} higher than 212 mW m^{-2} and 180 mW m^{-2} shown by MFCs with Co_3O_4 and MnO_2 cathodes, respectively. More complex materials were presented[148] whereby the Co_3O_4 nanoparticles were coated by nitrogen-doped NiFe-layered double hydroxides (LDH), forming a core–shell structure. The coating was performed using a hydrothermal technique. After deposition on stainless steel mesh, the obtained cathode used in the MFC setup delivered a maximum power density of 467.35 mW m^{-2}, 2.3 times higher than that of the cathode without a LDH-coating.

M. Kodali *et al.*[149] prepared a nanocomposite of iron amino antipyrine (Fe-AAPyr) with graphene nanosheets by the sacrificial support method using a silica template. Application of a nanocomposite in MFCs did not only result in a higher maximum power density of 2350 mW m^{-2}, compared to 2180 mW m^{-2} for Fe-AAPyr and 1500 mW m^{-2} for graphene nanosheets, but also a lower yield of H_2O_2. The study also highlighted the decrease in H_2O_2 yield with an increase in catalyst layer thickness (in the range between 0.2 and 0.6 mg cm^{-2}) due to its disproportionation within a thicker catalyst layer.

As biofouling is another undesirable phenomenon at the MFC cathode surface, components that inhibit bacterial growth, such as, *i.e.* silver, zinc or copper, are sometimes introduced into electrocatalytic nanocomposites.[150] For example, the composite of Cu_2O nanoparticles with reduced graphene oxide (rGO) was prepared by reducing the $Cu(Ac)_2$ supported on graphene oxide (GO) with diethylene glycol at 180 °C.[151] In the composite, rGO provided high surface area and excellent conductivity, while Cu_2O was a stable and cheap antimicrobial agent. The MFC equipped with the rGO/Cu_2O cathode exhibited an output voltage of 0.223 V. Due to antibacterial activity, more ORR active sites were exposed during the performance, resulting in better MFC operation. In another study, Co^{2+} atoms in Co_3O_4 spinel were replaced by Zn^{2+} to introduce antibacterial properties.[152] Due to the limited stability and conductivity of $ZnCo_2O_4$, its nanocomposite with GO was formed by the hydrothermal technique, followed by pyrolysis. After 1 mg cm^{-2} of the nanocomposite was deposited on carbon cloth, the resulting electrode exhibited a maximum power density of 773 mW m^{-2} in an MFC setup. Previous work[153] demonstrated that biofouling and decreased performance in an air cathode MFC treating human urine could be effectively addressed by a regeneration method involving alkaline lysis and cathode replacement, resulting in the recovery of the original power levels and suggesting its applicability for improved MFC operation in real-world settings.

In recent years, high ORR electrocatalytic activity was also discovered in the metallic centres in which metal atoms are coordinated by nitrogen atoms, forming Me-N_x domains. This way, single-atom catalysts (SACs) or few-atom metal clusters can be created, efficiently utilising metal atoms and leaving the axial position free for O_2 chemisorption.[154] In a study by X. Wang *et al.*,[155] atomically dispersed Fe–N_4 moieties were formed in hierarchically porous nitrogen-doped porous carbon (Fe-NpC). The sacrificial template method prepared the structure using histidine and agarose as nitrogen and carbon precursors. After pyrolysis with the sacrificial template (MgO + KCl), the template was etched, and the material was subjected to another pyrolysis process. Fe-NpC with a very high specific surface area of 1793 mW m^{-2} deposited on a carbon cloth substrate was used as an MFC cathode and showed a maximum power density of 1793 mW m^{-2}. This performance was higher than that of materials with Fe exchanged for Mn (889 mW m^{-2}) or Ni (610 mW m^{-2}). Still, in the latter cases, porous structures collapsed during the syntheses, resulting in much lower specific surface areas. In another study by K. Huang *et al.*,[156] atomic dispersion of Co atoms was achieved in N-doped mesoporous carbon. The material was obtained by liquid phase reduction by using hydrazine at −60 °C. This low temperature inhibited the nucleation of cobalt nanocrystals. The maximum power density of the single-atom catalyst used in the MFC cathode was 2550 mW m^{-2}, higher than *c.a.* 2200 mW m^{-2} achieved for the material synthesised by the same method but at room temperature that promoted the growth of cobalt nanocrystallites.

Also, S, N-doped carbon materials were enriched by Fe, Co or Ni nanoparticles.[157] The materials were obtained from biomass sources, namely chitosan and *p*-toluene sulfonic acid, by the hydrothermal method with the addition of the corresponding metal chloride, followed by freeze-drying and pyrolysis. The materials, possessing only *c.a.* 1 at% of metal on the surface, were used as MFC cathodes after deposition on titanium mesh. The system with an Fe-NSC cathode (2068 mW m^{-2}) showed the highest maximum power density in a series. This value was slightly higher than that of Co-NSC (1736 mW m^{-2}) and significantly higher than that of Ni-NSC (1441 mW m^{-2}). The low performance of Ni-NSC was explained by the inactivity of Ni–N centres in the ORR and higher H_2O_2 production yield. The same Ggoup also presented CoO/MgO nanoparticles encapsulated in porous N-carbon.[158] Due to the high graphitisation degree combined with a hierarchical porous structure and increased activity of Co-N_x active centres, the electrode, with the material deposited on titanium mesh, showed the maximum power density of 2258 mW m^{-2} in an MFC setup.

3.2.3. Conductive polymers and their composites. Typical conductive polymers include polyacetylene (PA), polyaniline (PANI), polypyrrole (PPy), polythiophene (PTH) and others.[159] Conducting polymers consist of localised and delocalised states, and the delocalisation of π bonds depends heavily upon disorder. This delocalisation is essential in generating charge carriers like polarons, bipolarons, solitons, *etc.*, responsible for the transition from the insulator to the metal. In their pure form, conjugate polymers function as an insulator for a semiconductor, and the conductivity increases with dopant concentration.[160]

Four different types of conductive polymers like polyaniline (PANI) and its co-polymers poly (aniline-co-*o*-aminophenol) (PANOA), poly (aniline-co-2,4-diaminophenol) (PANDAP) and

Table 3 Performance of MFCs equipped with different NP-containing cathodes

Cathode		Anode	Fold change of power output improvement[a]	Reference cathode material	Type of inoculum	Power output (mW m^{-2})	Ref.
Support material	Functionalisation						
Carbon-based metal-free materials							
Carbon cloth	N-doped carbon-aerogel	Carbon cloth	0.997	Pt/C	Exoelectrogenic bacteria	1048	134
Carbon-based support	N-doped carbon-based aerogel	Carbon paper	134	Pt/carbon paper	Mixed culture of bacteria	2.56	143
Roll-pressed CB/PTFE	KOH activated N-doped carbon aerogel	Carbon brush	3.84	Carbon aerogel	Sewage from treatment plant	967	144
Rotating graphite fiber brush	NP-co doped carbon	Graphite fiber brush	1.8	N and P co-doped carbon onto a graphite fiber brush air cathode	n.s[b]	879	133
Stainless steel mesh (SS)	Activated carbon with 15% rGO	Carbon fiber brush	1.35	Activated carbon	n.s[b]	2642	141
Metal-based materials and their composites							
CF	Ni/NiO_x nanoparticles	CF	3.33	Pt/C	Anaerobic sludge	1630	145
Carbon cloth	carbon/CoO–NiO	Carbon felt	12.33	Carbon	Anaerobic mix consortia	703	146
Stainless steel mesh (SS)	NiFe- layered double hydroxide@Co_3O_4	Graphite felt	2.27	Co_3O_4	Anaerobic activated sludge	467	148
AC/PTFE	Fe-AAPyr-2-GNS-2	Carbon brushes	2.28	Activated carbon	Activated sludge	235 μW cm^{-2}	149
Carbon cloth/CB/PTFE	Cu_2O/rGO	Carbon fiber brush	n.s[b]	Pt/C	Activated sludge	n.s[b]	151
Teflonized carbon cloth	GO–Zn/Co oxide	Carbon cloth	1.04	Pt/C	*S. oneidensis*	773	152
Carbon cloth/PTFE/CB	Fe-NpC	Carbon cloth	1.95	Pt/C	Anaerobic bacteria	1793	155
Steel mesh	Co atoms on N-doped mesoporous carbon	Graphite fiber brush	1.63	Pt/C	Anaerobic bacteria	2550	156
Titanium mesh	FeNS-co doped carbon	Carbon felt	1.55	N-doped carbon	Municipal wastewater	2068	157
Rolled AC/PTFE	N-carbon encapsulated CoO/MgO	Carbon felt	1.58	N-doped carbon	Municipal wastewater	2258	158
Conductive polymers and their composites							
Carbon felt	PANDAP	Carbon felt	3.97	Carbon felt	Anaerobic digester sludge	140	161
Carbon cloth	Carbon black/PANI-nanofiber	Carbon cloth	5.28	Carbon black	Wastewater from sewage treatment plant	496	172
Graphite felt	PPY/AQS	Graphite felt	14.1	Graphite felt	*Shewanella oneidensis*	299.6	163
Metal–organic frameworks and derived materials							
Carbon cloth/PTFE	Ni-MOF-74	Carbon cloth	0.39	Pt/C	n.s[b]	446	165
Stainless steel mesh (SS)	Fe–N–C/MOF/AC	Graphite fiber brushes	n.s[b]	n.s[b]	Domestic wastewater	2140	166
Graphite felt	(Co–Zn) ZIF	Graphite fiber	1.84	Pt/C	Domestic wastewater	5.66 W m^{-3}	167
Graphite felt	(MOF) MIL-53 (Al) with PEDOT	Graphite felt	0.87	Pt/C	Domestic wastewater	4.78 W m^{-3}	168

[a] Fold change of power output improvement compared to the electrodes containing no NPs within the same study. [b] n.s.: non specified.

poly (aniline-1,8-diaminonaphthalene) (PANDAN) were applied to modify carbon felt as aerobic abiotic cathodes and biocathodes in microbial fuel cells (MFCs). Using these dopants improves the power densities for abiotic cathodes (max for PANDAP reached 140 mW m^{-2}) and biocathodes (maximum for PANDAN got 285 mW m^{-2}), which compared to that of an unmodified material, increased by 180% and 300%,[161] respectively. The synthesis paths significantly impact the MFC power production efficiency. The conductive polyaniline nanofibers have been synthesised by interfacial polymerisation and applied to prepare composite cathodes with carbon black. Considerable improvement in power density was observed when this composite cathode was used. The maximum power density of 185 mW m^{-2} for pristine PANI increased to 496 mW m^{-2} for the composite cathode.[162] The following example of the application of a conductive polymer as a cathode catalyst is polypyrrole (PPy). The PPy films were electropolymerised on a graphite cathode with 9,10-anthraquinone-2-sulfonic acid sodium salt (AQS). The MFC with the PPy/AQS-modified cathode exhibited the maximum power density of 299.6 mW m^{-2}, which increased by 14.1 times compared to that of the unmodified cathode.[163]

3.2.4. Metal–organic frameworks and derived materials. MOFs have several advantages including distinctive skeletons, large specific surface area and tuneable pore structure.[164] Due to the presence of unsaturated metal-ion active sites, MOFs are a great candidate for excellent electrochemical catalysts.[165] Ni-MOF-74 and Ni–N–C (Ni-MOF-74 subjected to pyrolysis treatment at different temperatures) have been employed as air–cathode catalysts in MFCs. Applying Ni-MOF-74 in MFCs, a maximum power density of 446 mW m^{-2} was obtained, close to that of the 800 Ni–N–C composite material.[165] This research demonstrated that Ni-MOF-74 could be considered a two-electron transfer ORR catalyst and offers a promising technique for preparing Ni–N–C for use as a preferable four-electron transfer ORR catalyst.[165] The MOF on the activated carbon (AC) enhanced the performance of working cathodes that produced 2780 mW m^{-2}.[166] Remarkable power densities were also achieved by applying 50 mM phosphate buffer (PBS) as an electrolyte; however, power decreased to 780 mW m^{-2} when domestic wastewater was used.[166] In another research, application of non-noble metal-based cathode catalysts in the form of Co–Zn-ZIF coated silica particles pyrolysed at 900 °C were prepared. The final material, Co–CNF, produced the highest current and power densities at 18 A m^{-3} and 5.66 mW m^{-3} [167]. The composite conductive polymer and MOF also promote cathode material for power production. Poly(3,4-ethylene dioxythiophene) (PEDOT) modified metal–organic framework (MOF) MIL-53 (Al) was also presented as an efficient electrocatalyst for enhanced cathode half-cell potential in MFC operation.[168] The PEDOT-MIL-operated MFC achieved a power production of 4.78 W m^{-3} in ferricyanide catholyte and 3.49 W m^{-3} in aerated tap water catholyte with a cost of $0.076.[168] The MOF could also be doped with Fe and N elements to create Fe_x-N@MOF. Here, by controlling the formation of Fe_3C, the physical and structural properties of porous carbon were altered, and active chemical sites with Fe species were formed to catalyse the ORR.[169] $Fe_{0.05}$-N@&MOF-DMFC showed an open-circuit voltage of 1.08 V and a maximum power density of 1299.37 mW m^{-2}. The performance of $Fe_{0.05}$-N@&MOF-DMFC was remarkably better than that of Pt/C-DMFC (0.90 V and 858.52 mW m^{-2}).[169] Ni-catecholate-based metal–organic framework (Ni-CAT MOF) was synthesised by a two-step hydrothermal method using NiCoAl- layered double hydroxide (LDH) nanosheets and carbon nanotubes (MWCNTs).

As can be seen, based on the literature review on MFC cathodic materials, despite the high theoretical activity of biotic MFC cathodes, composed of enzymes or microbes, their application is limited due to their low durability in polluted environments and high cost.[145,149,151] Furthermore, most of the described MFC setups possess air cathodes, rather than cathodes that consume oxygen dissolved in an electrolyte. This is usually motivated by the reduction of aeration costs and the decrease in internal resistance in the system due to the absence of membranes in the setup.[142,170] Among the recently presented abiotic cathode materials we observe the tendencies to (1) avoid the use of noble metals, (2) form nanocomposites of two or more components in which each component can serve other purposes (*i.e.* increasing the surface area, increasing the conductivity, biofouling prevention, or introduction of active sites), (3) minimise the metal use (application of MOF-derived materials or single-atom catalysts) and (4) replace the expensive carbon nanomaterials (such as rGO, GO or CNTs) with cheaper, nanoporous carbons that are more cost-effective.

Nevertheless, conditions in MFC systems remain challenging for engineering of ORR electrocatalysts. The main obstacles include the use of neutral or near-neutral (pH ~7) electrolytes in which the availability of both OH^- and H^+ is limited. Most of the ORR electrocatalysts performing in more mature technologies, such as PEM fuel cells, direct methanol fuel cells or alkaline fuel cells operate in alkaline or acidic media in which the ORR kinetics are higher.[137,149] Additional challenges for the ORR in MFCs include the biofouling effects and the inactivation of some of the highly electrocatalytically active sites by the reaction medium.[152,153,171] MFC engineering can benefit from the scientific advances in ORR electrocatalysis; however, further research is required with respect to durability of the electrode under operating conditions that can be detrimental to some classes of materials.[138]

Table 3 summarises the performance of MFCs equipped with different nanomaterial-containing cathodes.

4. Nanomaterials for a MFC separator membrane

4.1. Ideal properties of a separator membrane

Membrane material and the size of the membrane pore size distribution, impact the process of moving ions and decreasing oxygen transfer to the cathode. The membrane works as a physical separator, allowing cations to pass from the negative electrode to the positive electrode while preventing oxygen migration in the anode chamber from the cathode compartment.[24,27,45,59,173] MFC membranes must have low resistance, high cation/anion conductivity, high energy recovery, and

strong chemical and physical durability to avoid oxygen transfer from the cathode chamber to the anode chamber.[24,27]

One of the barriers to MFC commercialisation is the high PEM cost, with the exception of ceramic materials. Ceramic membranes used in MFCs, first reported in 2010 [174] have worked remarkably well as cost-effective alternatives to commercial ion selective membranes with higher power densities; this is a large and continuously growing topic in the area of BES but will not be expanded further herewith, as there already are some useful review papers on the topic.[175,176] Because of the significant expense of commercial PEMs, scientists have long been interested in replacing it with a less priced PEM.[27,59,173,177] Although commercial membranes are often preferred they regularly suffer from oxygen leakage from the cathode to the anode chamber, high costs, substrate crossover, cation transport and ion buildup.[24,178,179] Considering these drawbacks, current efforts focus on the development of novel PEMs which provide better performance.[27,59,180] In this section, PEMs including NMs are discussed. Table 4 summarises the performance of MFCs equipped with different nanomaterial-containing separators.

4.2. Separator membranes including nanomaterials

The standard materials used to fabricate electrodes and membranes are inadequate to enhance MFC efficiency.[24] The ratio of the PEM surface area to system volume is crucial for achieving maximum power performance. The employment of a nanomaterial with a significant specific surface area will cause the PEM to have a larger surface area.[178] Nanomaterials were employed in the manufacturing processes of membrane components, which enhanced the physical and chemical features of the membranes and increased cation transfer rates, however, introducing polymer or nanoparticles into polymeric membranes can drastically alter their original structure, mainly the intensity of roughness on their surface, and a rougher surface encourages membrane biofouling.[27,47]

The current practice is to increase membrane performance, and physical and thermal characteristics by inserting nanomaterials into membrane designs, which helps in obtaining targeted characteristics and enhancing MFC efficiency.[24] Nanoparticles increase separation performance by providing preferred permeation routes, preventing unwanted species from passing, and boosting thermal and mechanical characteristics.[24,59,173,197] By interfering with characteristics including proton conductivity, oxygen cross-over, water absorption, separation, and anti-fouling, the use of nanomaterials in membranes can help the system operate more efficiently.[198] The nanocomposite materials in the membranes reduce the pore size and roughness of the membranes, creating high resistance

Table 4 Performance of MFCs equipped with different NP-containing separators

Membrane		Fold change of power output improvement[a]	Type of inoculum	Power output (mW m^{-2})	Ref.
Support material	Functionalisation				
Carbon-based nanomaterials					
Nafion	CNF	3.39	Yeast	47.48	181
Nafion	Activated carbon nanofiber	4.12	Yeast	57.64	181
Poly-3-hydroxyalkanoates (PHA)	MWCNT	—	Mixed inoculum	361	182
Chitosan	MWCNT	1.23	*Escherichia coli*	46.94	183
Sulfonated poly(ether ether ketone) (SPEEK)	CNTs	2.15	Mixed inoculum	1.77	184
Metal-based nanomaterials					
Poly ether sulfone (PES)	Fe_3O_4	1.29	*S. cerevisiae*	20	185
Sulfonated polyether ether ketone (SPEK)	AgGO	1.29	Mixed inoculum	896	186
Sulphonated polystyrene ethylene butylene polystyrene (SPSEBS)	Sulphonated zinc oxide nanorods (SZnO NR)	1.21	Mixed inoculum	147	187
PES	Fe_3O_4	119.87	n.s[c]	9.59	188
SPEK	Fe_3O_4	2.21	*Escherichia coli*	104	48
Sulfonated polyethersulfone (SPES)	GO	—	Mixed inoculum	101.2	189
Polymer-based nanomaterials					
Polyvinylidene fluoride (PVDF)	Nafion	1.68	Yeast	4.9	190
Medium-chain-length polyhydroxyalkanoates (mcl-PHA)	PHB	2	*Escherichia coli*	601	191
PVDF	Perfluorinated sulfuric acid ionomer	1.27[b]	*Shewanella oneidensis*	548	192
Bacterial nanocellulose (BNC)	Lignin	2.72	*Escherichia coli*	18.5	193
Other nanomaterials					
SPEEK	Montmorillonite	1.13	*Escherichia coli*	55.68	194
SPEEK	Goethite	n.s[c]	n.s[c]	73.7	195
SPEEK	Sulfonated SiO_2	1.48	Mixed inoculum	1008	196

[a] Fold change of power output improvement compared to the electrodes containing no NPs within the same study. [b] Value estimated from figures. [c] n.s.: non-specified.

to inter-sectional oxygen flow and noticeable rise in proton-exchange tendency with high coulombic efficiency, resulting in power output,[178] hence boosting the productivity and effectiveness of MFCs in producing electricity and optimising wastewater treatment.[24] In a study examining the performance of MFCs with machine learning, it was found that nanocomposite membranes can provide higher power density than commercial membrane alternatives.[199]

4.2.1. Carbon nanomaterials. Carbon nanomaterials boost power output by altering the membrane's porosity, pore size, and roughness in MFCs. These nanocomposite membranes' smaller pores and rougher surface prevent components like bacteria from moving from the anode to the cathode and inhibit oxygen from moving from the cathode to the anode. Furthermore, due to the inherent nature of carbon nanofibers (CNFs), decreased roughness improves the membrane's conductivity while reducing fouling issues.[27,181] Due to the aforementioned attributes, carbon nanotubes (CNTs) have emerged as a brand-new type of enhanced inorganic filler.[197] A higher power output was produced when CNF/Nafion and activated-CNF/Nafion membranes were applied to MFCs, demonstrating that MFCs may be made to generate a higher power output with membranes other than Nafion 117 and Nafion 112.[181]

Graphene oxide (GO) has a wide range of possible uses with its large surface area. Graphene also has a high mechanical strength, excellent electrical and thermal conductivity, and a high specific surface area. Together with the fact that it is an excellent insulator, this gives GO a lot of promise in applications. In fact, due to the lack of a proton-exchange group, natural GO did not boost the effectiveness of PEMs as much as anticipated. Functionalized GO may have the potential to make a more significant contribution.[197,200]

4.2.2. Metal based nanomaterials. Several investigations have been performed to examine the utilization of Fe_3O_4 nanoparticles to boost the physicochemical characteristics and separation efficiency of polymeric membranes, and it has been demonstrated that the use of Fe_3O_4 nanoparticles for improving the properties of IEMs is also possible.[200] Magnetite ($FeO \cdot Fe_2O_3$ or Fe_3O_4) has a unique liquid proton hopping mechanism that improves proton conductivity *via* hydrogen migration. When MFCs were tested with a Fe_3O_4 enriched membrane, power density increased, and oxygen diffusion decreased.[48]

Titania (TiO_2) is a unique semiconductor with photocatalytic and hydrophilic features. Titania near the surface reduces fouling better than other surface-bound nanoparticles. It has the potential to minimize hydrophobic connections between membrane surfaces and bacteria.[27,201] Furthermore, TiO_2 antibacterial capabilities aid in improved membrane antifouling performance, which leads to improved MFC performance since biofilm growth on membrane surfaces negatively affects proton conductivity.[202]

As already mentioned, MOFs are also suitable as a PEM material, due to high porosity which can create channels for protons to travel through. To supply sufficient contacts for proton exchange in the MFC process, MOF materials have a large effective surface area that can hold plenty of acid groups and water molecules.[197] Despite receiving a lot of attention for their excellent proton conductivity, MOFs are extremely challenging to directly process for fuel cells because of their unique and varied crystal structures. The most effective technique to address this issue is to hybridize MOFs with other polymers to create composite membranes.[203] As a result of interactions between the many hydrogen bonds in MOFs and the polymer matrix, a denser hydrogen bond structure and more proton transport pathways are created. The limited cavities of MOFs also reduce fuel and oxidant diffusion and increases selectivity.[197]

Silver nanoparticles, a sophisticated nanomaterial, demonstrate effectiveness as additives in sulphonated poly ether ether ketone (SPEEK) membranes. They have shown the potential to mitigate membrane biofouling during extended operation of MFC equipment.[204,205]

5. Conclusions and future prospects

This review comprehensively discusses the current status of nanocomposites used in MFCs. Achieving a commercialised and sustainable MFC system involves addressing two crucial challenges. The first challenge pertains to the cost associated with setting up an MFC, which can be a significant barrier to entry for many companies. The second challenge is ensuring that the component materials are suitable for the MFC system, as this plays a vital role in determining its economic feasibility. Overcoming these challenges is necessary to realise the potential of MFC technology and establish it as a viable option for widespread adoption. The electrodes and separator are critical components with regard to both sustainability and cost. Improved power output and cost-effective materials with a new design can be used in industrial scale applications. The efficiency of MFCs largely depends on the properties of the electrode material used in the system. Several desirable electrode properties have been identified in this review, including high electrical conductivity, porosity, large surface area, durability, biocompatibility, low cost, and high catalytic activity. Nanomaterials exhibit a high specific surface area to volume ratio, tunable surface charge, and excellent electron transport properties that can enhance electron transfer kinetics between the microorganisms and the electrode surface, thereby improving the efficiency of the MFC. In particular, zero-dimensional nanomaterials (spheres or quasi-spheres with a diameter $\leq$100 nm), as well as one-dimensional counterparts (nanowires, nanorods, nanofibers, and nanotubes), which provide MFC components with numerous active edge sites per unit mass (the smaller the nanostructure, the larger the site number), boost their catalytic performance, electron transfer and a reduction in internal resistance, ultimately leading to increased power generation. Conversely, two-dimensional nanomaterials, characterised by single or few atomic layers, offer MFC components a substantial surface area (the larger the 2D extent, the greater the surface area), translating into enhanced electrical conductivity, favourable biocompatibility, durability, and mechanical stability. In contrast, three-dimensional nanomaterials, known for their hierarchical or macroporous structures, facilitate the immobilisation of microorganisms on the electrode surface

while effectively mitigating issues related to biofouling, thus improving bacterial electroactivity capitalization. As emphasised throughout this manuscript, the careful selection, integration, and optimization of nanomaterials can harness these properties, preserving the MFC components' structural integrity and ensuring consistent performance, ultimately extending their lifespan and enhancing performance reproducibility.

Carbon nanostructures remain the most commonly used materials for both anode and cathode electrodes in MFCs because of their affordability, high biocompatibility, and desirable structural features (porosity and surface area). CNTs offer a significant advantage with their large active surface area and rGO exhibits conductivity and hydrophilicity, while CNPs can be produced in a cheap and eco-friendly way using waste products. All the cited studies in this review show that the conductivity of carbon-based nanoparticles can be significantly improved by the addition of metals and polymers to form nanocomposites, resulting in exceptional performance in terms of power density and substrate oxidation. However, it should be noted that while metal nanoparticles exhibit high conductivity, they are costly and exhibit poor biocompatibility for EB. In contrast, conductive polymers, which are extensively used, offer superior biocompatibility and lower cost but are less conductive. Research on the use of nanocomposites to improve MFC performance is still in its early stages. Further studies are required to fill research gaps in our knowledge, with a focus on:

(1) Optimising the uniformity and composition of the coating. To achieve optimal EET between the catalytic biofilm and the anode surface and to ensure good mass and electron transfer, it is essential to ensure homogeneous dispersal of carbon, metal, or polymer nanoparticles in the supporting electrode material.

(2) Investigating the long-term operational stability and reproducibility of MFCs equipped with innovative electrode nanomaterials.

(3) Exploring EET mechanisms and how they can be improved by nanomaterials. Most of the studies highlighted an improvement in performance due to a higher EET, but the fundamentals of this mechanism remain largely unknown.

The use of nanomaterials in MFCs holds significant potential for advancing the development of sustainable and efficient energy generation technologies. In conclusion, the incorporation of nanomaterials in MFC components appears to be more viable than traditional materials for designing the desirable electrode properties of MFC systems. This will aid in improving the efficiency of MFCs while effectively addressing long-term sustainability concerns.

It is important to note that the majority of papers cited in this review only quote the derived power density, without disclosing the actual surface area of the electrode used in the experiments or the absolute power values. This lack of information hinders the understanding of the capability or practical applicability of the subject systems and it represents a common deficiency in reporting performance levels – this is the main reason why a direct comparison has not been attempted in this study. As part of future developments, it would be important for researchers to include both actual and normalized power values when reporting their findings.

Author contributions

Fatma Yalcinkaya and Ioannis Ieropoulos: conceptualization, methodology, supervision, data curation, writing – original draft, preparation, writing – review & editing, visualization. Karolina Kordek-Khalil, Esra Altiok, Anna Salvian, Anna Siekierka, Rafael Omar Torres Mendieta, Claudio Avignone-Rossa, Andrea Pietrelli, and Siddharth Gadkari: conceptualization, methodology, data curation, writing – original draft, preparation, writing – review & editing, visualization.

Conflicts of interest

There are no conflicts to declare.

Acknowledgements

This article is based upon work from COST Action [Protection, Resilience, Rehabilitation of damaged environment (PHOENIX), CA19123], supported by COST (European Cooperation in Science and Technology; **https://www.cost.eu**). The authors acknowledge the COST Action Horizon program and the COST Action PHOENIX: Protection, resilience, rehabilitation of damaged environment (CA19123). The author E. A. acknowledges the International Mobilities at the TUL II, CZ.02.2.69/0.0/0.0/18_053/0017628, Czech Republic. The author IAI is a Bill & Melinda Gates Foundation grantee (grant no.: INV 042655).

References

1 F. S. Fadzli, S. A. Bhawani and R. E. Adam Mohammad, *J. Chem.*, 2021, **2021**, 1–16.
2 T. Z. Kaya, E. Altıok, E. Güler and N. Kabay, *Membranes*, 2022, **12**, 1240.
3 S. Pandit, K. Chandrasekhar, R. Kakarla, A. Kadier and V. Jeevitha, *Microbial Applications*, Bioremediation and Bioenergy, 2017, vol. 1, pp. 165–188.
4 A. Priya, C. Subha, P. S. Kumar, R. Suresh, S. Rajendran, Y. Vasseghian and M. Soto-Moscoso, *Environ. Res.*, 2022, **210**, 112930.
5 A. Siekierka, F. Yalcinkaya and M. Bryjak, *J. Environ. Chem. Eng.*, 2023, **11**, 110145.
6 S. Hadian and K. Madani, *Ecol. Indic.*, 2015, **52**, 194–206.
7 R. Kothari, V. V. Tyagi and A. Pathak, *Renewable Sustainable Energy Rev.*, 2010, **14**, 3164–3170.
8 I. Iavicoli, V. Leso, W. Ricciardi, L. L. Hodson and M. D. Hoover, *Environ. Health*, 2014, **13**, 78.
9 F. Almeshqab and T. S. Ustun, *Renewable Sustainable Energy Rev.*, 2019, **102**, 35–53.
10 D. Kundu, D. Dutta, P. Samanta, S. Dey, K. C. Sherpa, S. Kumar and B. K. Dubey, *Sci. Total Environ.*, 2022, **848**, 157709.

11 H. Gul, W. Raza, J. Lee, M. Azam, M. Ashraf and K.-H. Kim, *Chemosphere*, 2021, **281**, 130828.
12 R. K. Yadav, S. Das and S. A. Patil, *Trends Biotechnol.*, 2023, **41**, 484–496.
13 V. Raja, S. Dutta, P. Murugesan, J. A. Moses and C. Anandharamakrishnan, *Environ. Chem. Lett.*, 2023, **21**, 839–864.
14 S. Dilip Kumar, M. Yasasve, G. Karthigadevi, M. Aashabharathi, R. Subbaiya, N. Karmegam and M. Govarthanan, *Chemosphere*, 2022, **287**, 132439.
15 K. Rabaey and R. A. Rozendal, *Nat. Rev. Microbiol.*, 2010, **8**, 706–716.
16 R. Gautam, J. K. Nayak, N. V. Ress, R. Steinberger-Wilckens and U. K. Ghosh, *Chem. Eng. J.*, 2023, **455**, 140535.
17 B. E. Logan, R. Rossi, A. Ragab and P. E. Saikaly, *Nat. Rev. Microbiol.*, 2019, **17**, 307–319.
18 H. Bennetto, *Biotechnol. Educ.*, 1990, **1**, 163–168.
19 M. C. Potter, *Proc. R. Soc. London, Ser. B*, 1911, **84**, 260–276.
20 M. Ramya and P. Senthil Kumar, *Chemosphere*, 2022, **288**, 132512.
21 W. Apollon, I. Rusyn, N. González-Gamboa, T. Kuleshova, A. I. Luna-Maldonado, J. A. Vidales-Contreras and S.-K. Kamaraj, *Sci. Total Environ.*, 2022, **817**, 153055.
22 Y. Liu, S. Guo, J. Wang and C. Li, *J. Environ. Chem. Eng.*, 2022, **10**, 107918.
23 D. Guo, H.-F. Wei, R.-B. Song, J. Fu, X. Lu, R. Jelinek, Q. Min, J.-R. Zhang, Q. Zhang and J.-J. Zhu, *Nano Energy*, 2019, **63**, 103875.
24 N. K. Abd-Elrahman, N. Al-Harbi, N. M. Basfer, Y. Al-Hadeethi, A. Umar and S. Akbar, *Molecules*, 2022, **27**, 7483.
25 R. Fogel and J. L. Limson, in *Nanomaterials for Fuel Cell Catalysis*, ed. K. I. Ozoemena and S. Chen, Springer International Publishing, Cham, 2016, pp. 551–575.
26 Y.-J. Jiang, S. Hui, L.-P. Jiang and J.-J. Zhu, *Chem.–Eur. J.*, 2023, **29**, e202202002.
27 S. Narayanasamy and J. Jayaprakash, in *Nanotechnology in Fuel Cells*, ed. H. Song, T. A. Nguyen and G. Yasin, Elsevier, 2022, pp. 139–171.
28 A. Chaturvedi, S. K. Dhillon and P. P. Kundu, *Sustain. Energy Technol. Assess.*, 2022, **53**, 102479.
29 B. Virdis and P. G. Dennis, *J. Power Sources*, 2017, **356**, 556–565.
30 H. Matabosch Coromina, G. Antonio Cuffaro, T. Tommasi, S. Puig and B. Virdis, *J. Electroanal. Chem.*, 2022, **920**, 116546.
31 M. T. Noori, C. I. Ezugwu, Y. Wang and B. Min, *J. Power Sources*, 2022, **547**, 231947.
32 X. Lin, L. Zheng, M. Zhang, Y. Qin, X. Liu, Y. Liu, H. Li and C. Li, *Chem. Eng. J.*, 2023, **453**, 139910.
33 F. Cui, W. Wang, C. Liu, X. Chen and N. Li, *Int. J. Energy Res.*, 2020, **44**, 4426–4437.
34 A. J. Slate, N. A. Hickey, J. A. Butler, D. Wilson, C. M. Liauw, C. E. Banks and K. A. Whitehead, *J. Power Sources*, 2021, **499**, 229938.
35 Z. Zhang, M. A. Sadeghi, R. Jervis, S. Ye, J. T. Gostick, J. E. Barralet and G. Merle, *Adv. Funct. Mater.*, 2019, **29**, 1903983.
36 L. Xiao, J. Damien, J. Luo, H. D. Jang, J. Huang and Z. He, *J. Power Sources*, 2012, **208**, 187–192.
37 T. Wilberforce, M. A. Abdelkareem, K. Elsaid, A. G. Olabi and E. T. Sayed, *Energy*, 2022, **240**, 122478.
38 Y. Du, F.-X. Ma, C.-Y. Xu, J. Yu, D. Li, Y. Feng and L. Zhen, *Nano Energy*, 2019, **61**, 533–539.
39 S. Rojas-Flores, E. Ramirez-Asis, J. Delgado-Caramutti, R. Nazario-Naveda, M. Gallozzo-Cardenas, F. Diaz and D. Delfin-Narcizo, *Sustainability*, 2023, **15**, 3651.
40 A. J. Slate, K. A. Whitehead, D. A. C. Brownson and C. E. Banks, *Renewable Sustainable Energy Rev.*, 2019, **101**, 60–81.
41 A. AlSayed, M. Soliman and A. Eldyasti, *Renewable Sustainable Energy Rev.*, 2020, **134**, 110367.
42 H. Pham, N. Boon, M. Marzorati and W. Verstraete, *Water Res.*, 2009, **43**, 2936–2946.
43 M. Rosenbaum, F. Aulenta, M. Villano and L. T. Angenent, *Bioresour. Technol.*, 2011, **102**, 324–333.
44 K. Obileke, H. Onyeaka, E. L. Meyer and N. Nwokolo, *Electrochem. Commun.*, 2021, **125**, 107003.
45 A. Pietrelli, A. Micangeli, V. Ferrara and A. Raffi, *Sustainability*, 2014, **6**, 7263–7275.
46 P. M. D. Serra, A. Espírito-Santo and M. Magrinho, *Instrum. Exp. Tech.*, 2020, **63**, 567–576.
47 J. X. Leong, W. R. W. Daud, M. Ghasemi, K. B. Liew and M. Ismail, *Renewable Sustainable Energy Rev.*, 2013, **28**, 575–587.
48 N. V. Prabhu and D. Sangeetha, *Chem. Eng. J.*, 2014, **243**, 564–571.
49 J. Greenman, I. A. Ieropoulos and C. Melhuish, *Applications of Electrochemistry and Nanotechnology in Biology and Medicine I*, 2011, pp. 239–290.
50 K. A. Dwivedi, S.-J. Huang, C.-T. Wang and S. Kumar, *Chemosphere*, 2022, **288**, 132446.
51 A. Nawaz, I. ul Haq, K. Qaisar, B. Gunes, S. I. Raja, K. Mohyuddin and H. Amin, *Process Saf. Environ. Prot.*, 2022, **161**, 357–373.
52 P. Shanmuganathan, P. Rajasulochana and A. Ramachandra, *Int. J. Mech. Eng. Technol.*, 2018, **9**, 137–148.
53 A. Pietrelli, I. Bavasso, N. Lovecchio, V. Ferrara and B. Allard, in *2019 IEEE 8th International Workshop on Advances in Sensors and Interfaces*, IWASI, 2019, pp. 302–306.
54 N. Lovecchio, V. Di Meo and A. Pietrelli, *Bioengineering*, 2023, **10**(5), 624.
55 V. B. Wang, J. Du, X. Chen, A. W. Thomas, N. D. Kirchhofer, L. E. Garner, M. T. Maw, W. H. Poh, J. Hinks, S. Wuertz, S. Kjelleberg, Q. Zhang, J. S. C. Loo and G. C. Bazan, *Phys. Chem. Chem. Phys.*, 2013, **15**, 5867–5872.
56 T. Chen, C. Zou, J. Pan, M. Wang, L. Qiao, F. Wang, Q. Zhao, H. Cheng, C. Ding and Y. Yuan, *Processes*, 2022, **10**, 179.
57 R. Selvasembian, J. Mal, R. Rani, R. Sinha, R. Agrahari, I. Joshua, A. Santhiagu and N. Pradhan, *Bioresour. Technol.*, 2022, **346**, 126462.
58 C. Donovan, A. Dewan, H. Peng, D. Heo and H. Beyenal, *J. Power Sources*, 2011, **196**, 1171–1177.

59 M. Rahimnejad, G. Bakeri, G. Najafpour, M. Ghasemi and S.-E. Oh, *Biofuel Res. J.*, 2014, **1**, 7–15.
60 A. Shantaram, H. Beyenal, R. R. A. Veluchamy and Z. Lewandowski, *Environ. Sci. Technol.*, 2005, **39**, 5037–5042.
61 A. Tsipa, C. K. Varnava, P. Grenni, V. Ferrara and A. Pietrelli, *Processes*, 2021, **9**, 1038.
62 V. Ancona, A. B. Caracciolo, D. Borello, V. Ferrara, P. Grenni and A. Pietrelli, *Int. J. Environ. Res. Impacts*, 2020, **3**, 168–179.
63 I. Gajda, J. Greenman and I. A. Ieropoulos, *Curr. Opin. Electrochem.*, 2018, **11**, 78–83.
64 R. Kumar, L. Singh, A. Zularisam and F. I. Hai, *Int. J. Energy Res.*, 2018, **42**, 369–394.
65 C. Santoro, C. Arbizzani, B. Erable and I. Ieropoulos, *J. Power Sources*, 2017, **356**, 225–244.
66 A. Baudler, I. Schmidt, M. Langner, A. Greiner and U. Schröder, *Energy Environ. Sci.*, 2015, **8**, 2048–2055.
67 L. Gonzalez Olias, P. J. Cameron and M. Di Lorenzo, *Front. Energy Res.*, 2019, **7**, 105.
68 K. Guo, S. Freguia, P. G. Dennis, X. Chen, B. C. Donose, J. Keller, J. J. Gooding and K. Rabaey, *Environ. Sci. Technol.*, 2013, **47**, 7563–7570.
69 R. S. Renslow, J. T. Babauta, P. D. Majors and H. Beyenal, *Energy Environ. Sci.*, 2013, **6**, 595–607.
70 J. Wei, P. Liang and X. Huang, *Bioresour. Technol.*, 2011, **102**, 9335–9344.
71 B. Li, J. Zhou, X. Zhou, X. Wang, B. Li, C. Santoro, M. Grattieri, S. Babanova, K. Artyushkova and P. Atanassov, *Electrochim. Acta*, 2014, **134**, 116–126.
72 M. Masoudi, M. Rahimnejad and M. Mashkour, *Electrochim. Acta*, 2020, **344**, 136168.
73 A. A. Yaqoob, M. N. Mohamad Ibrahim, M. Rafatullah, Y. S. Chua, A. Ahmad and K. Umar, *Materials*, 2020, **13**, 2078.
74 B. C. Steele and A. Heinzel, *Nature*, 2001, **414**, 345–352.
75 J. M. Sonawane, A. Yadav, P. C. Ghosh and S. B. Adeloju, *Biosens. Bioelectron.*, 2017, **90**, 558–576.
76 Y. Liu, X. Zhang, Q. Zhang and C. Li, *Energy Technol.*, 2020, **8**, 2000206.
77 S. Li, C. Cheng, H. Liang, X. Feng and A. Thomas, *Adv. Mater.*, 2017, **29**, 1700707.
78 H. Wang and S. Tao, *Nanoscale Adv.*, 2021, **3**, 2280–2286.
79 M. Kamali, T. M. Aminabhavi, R. Abbassi, R. Dewil and L. Appels, *Fuel*, 2022, **310**, 122347.
80 X. Fan, Y. Zhou, X. Jin, R.-B. Song, Z. Li and Q. Zhang, *Carbon Energy*, 2021, **3**, 449–472.
81 L. Huang, J. M. Regan and X. Quan, *Bioresour. Technol.*, 2011, **102**, 316–323.
82 H.-Y. Tsai, C.-C. Wu, C.-Y. Lee and E. P. Shih, *J. Power Sources*, 2009, **194**, 199–205.
83 B. E. Logan, B. Hamelers, R. Rozendal, U. Schröder, J. Keller, S. Freguia, P. Aelterman, W. Verstraete and K. Rabaey, *Environ. Sci. Technol.*, 2006, **40**, 5181–5192.
84 Y. Shen, M. Wang, I. S. Chang and H. Y. Ng, *Bioresour. Technol.*, 2013, **136**, 707–710.
85 W. Yang, J. Li, Q. Fu, L. Zhang, Z. Wei, Q. Liao and X. Zhu, *Renewable Sustainable Energy Rev.*, 2021, **136**, 110460.
86 N. Xiao, R. Wu, J. J. Huang and P. R. Selvaganapathy, *Chem. Eng. Sci.*, 2020, **221**, 115691.
87 J. Yang, S. Cheng, Y. Sun and C. Li, *Biotechnol. Lett.*, 2017, **39**, 1515–1520.
88 M. Yellappa, J. S. Sravan, O. Sarkar, Y. V. R. Reddy and S. V. Mohan, *Bioresour. Technol.*, 2019, **284**, 148–154.
89 Y. Wang, X. Pan, Y. Chen, Q. Wen, C. Lin, J. Zheng, W. Li, H. Xu and L. Qi, *J. Appl. Electrochem.*, 2020, **50**, 1281–1290.
90 Q. Yang, X. Zhao, J. Yang, B. Zhou, J. Wang, Y. Dong and H. Zhao, *Int. J. Hydrogen Energy*, 2019, **44**, 20304–20311.
91 Y. Qiao, C. M. Li, S.-J. Bao and Q.-L. Bao, *J. Power Sources*, 2007, **170**, 79–84.
92 A. Olabi, T. Wilberforce, E. T. Sayed, K. Elsaid, H. Rezk and M. A. Abdelkareem, *Sci. Total Environ.*, 2020, **749**, 141225.
93 L. Zeng, W. Zhang, P. Xia, W. Tu, C. Ye and M. He, *Biosens. Bioelectron.*, 2018, **102**, 351–356.
94 A. Kaur, S. Ibrahim, C. J. Pickett, I. S. Michie, R. M. Dinsdale, A. J. Guwy and G. C. Premier, *Sens. Actuators, B*, 2014, **201**, 266–273.
95 F. Bensalah, J. Pézard, N. Haddour, M. Erouel, F. Buret and K. Khirouni, *Nanomaterials*, 2021, **11**, 3144.
96 D. R. Lovley, J. D. Coates, E. L. Blunt-Harris, E. J. P. Phillips and J. C. Woodward, *Nature*, 1996, **382**, 445–448.
97 R. Wang, M. Yan, H. Li, L. Zhang, B. Peng, J. Sun, D. Liu and S. Liu, *Adv. Mater.*, 2018, **30**, 1800618.
98 C. J. Kirubaharan, K. Santhakumar, G. G. kumar, N. Senthilkumar and J.-H. Jang, *Int. J. Hydrogen Energy*, 2015, **40**, 13061–13070.
99 W. Lv, Z. Li, Y. Deng, Q.-H. Yang and F. Kang, *Energy Stor. Mater.*, 2016, **2**, 107–138.
100 A. ElMekawy, H. M. Hegab, D. Losic, C. P. Saint and D. Pant, *Renewable Sustainable Energy Rev.*, 2017, **72**, 1389–1403.
101 N. Yang, Y. Ren, X. Li and X. Wang, *Nanomaterials*, 2016, **6**(9), 174.
102 J. Ma, N. Shi, Y. Zhang, J. Zhang, T. Hu, H. Xiao, T. Tang and J. Jia, *J. Power Sources*, 2020, **450**, 227628.
103 S. Singh, P. K. Bairagi and N. Verma, *Electrochim. Acta*, 2018, **264**, 119–127.
104 Y. Yuan, S. Zhou, N. Xu and L. Zhuang, *Appl. Microbiol. Biotechnol.*, 2011, **89**, 1629–1635.
105 K. Zhu, S. Wang, H. Liu, S. Liu, J. Zhang, J. Yuan, W. Fu, W. Dang, Y. Xu, X. Yang and Z. Wang, *J. Cleaner Prod.*, 2022, **336**, 130374.
106 Y.-Y. Yu, C. X. Guo, Y.-C. Yong, C. M. Li and H. Song, *Chemosphere*, 2015, **140**, 26–33.
107 C. Dumas, R. Basseguy and A. Bergel, *Electrochim. Acta*, 2008, **53**, 5235–5241.
108 E. Guerrini, P. Cristiani, M. Grattieri, C. Santoro, B. Li and S. Trasatti, *J. Electrochem. Soc.*, 2013, **161**, H62.
109 M. Sun, F. Zhang, Z.-H. Tong, G.-P. Sheng, Y.-Z. Chen, Y. Zhao, Y.-P. Chen, S.-Y. Zhou, G. Liu, Y.-C. Tian and H.-Q. Yu, *Biosens. Bioelectron.*, 2010, **26**, 338–343.
110 X. Wu, X. Xiong, G. Owens, G. Brunetti, J. Zhou, X. Yong, X. Xie, L. Zhang, P. Wei and H. Jia, *Bioresour. Technol.*, 2018, **270**, 11–19.
111 H. Xu, X. Quan, Z. Xiao and L. Chen, *Chem. Eng. J.*, 2018, **335**, 539–547.

112 S. Singh and N. Verma, *Int. J. Hydrogen Energy*, 2015, **40**, 1145–1153.
113 S. Murthy, P. Effiong and C. C. Fei, in *Metal Oxide Powder Technologies*, ed. Y. Al-Douri, Elsevier, 2020, pp. 233–251.
114 B. Tripathi, S. Pandit, A. Sharma, S. Chauhan, A. S. Mathuriya, P. K. Dikshit, P. K. Gupta, R. C. Singh, M. Sahni, K. Pant and S. Singh, *Catalysts*, 2022, **12**, 1040.
115 J. Tang, Y. Yuan, T. Liu and S. Zhou, *J. Power Sources*, 2015, **274**, 170–176.
116 K. Tahir, W. Miran, J. Jang, N. Maile, A. Shahzad, M. Moztahida, A. A. Ghani, B. Kim and D. S. Lee, *Chemosphere*, 2021, **265**, 129098.
117 E. Antolini, *Biosens. Bioelectron.*, 2015, **69**, 54–70.
118 M. R. Haider, W.-L. Jiang, J.-L. Han, H. M. A. Sharif, Y.-C. Ding, H.-Y. Cheng and A.-J. Wang, *Appl. Catal., B*, 2019, **256**, 117774.
119 I. Lascu, C. Locovei, C. Bradu, C. Gheorghiu, A. M. Tanase and A. Dumitru, *Int. J. Mol. Sci.*, 2022, **23**, 11230.
120 Y. Song, Z. Qin, Z. Huang, T. Liu, Y. Li and X.-X. Liu, *J. Mater. Res.*, 2018, **33**, 1109–1119.
121 B. Lai, X. Tang, H. Li, Z. Du, X. Liu and Q. Zhang, *Biosens. Bioelectron.*, 2011, **28**, 373–377.
122 C. Li, L. Zhang, L. Ding, H. Ren and H. Cui, *Biosens. Bioelectron.*, 2011, **26**, 4169–4176.
123 R.-B. Song, K. Yan, Z.-Q. Lin, J. S. C. Loo, L.-J. Pan, Q. Zhang, J.-R. Zhang and J.-J. Zhu, *J. Mater. Chem. A*, 2016, **4**, 14555–14559.
124 X. Liu, X. Zhao, Y.-Y. Yu, Y.-Z. Wang, Y.-T. Shi, Q.-W. Cheng, Z. Fang and Y.-C. Yong, *Electrochim. Acta*, 2017, **255**, 41–47.
125 B. Balli, A. Şavk and F. Şen, in *Nanocarbon and Its Composites*, ed. A. Khan, M. Jawaid, Dr. Inamuddin and A. M. Asiri, Woodhead Publishing, 2019, pp. 123–151.
126 C. Zhao, J. Wu, S. Kjelleberg, J. S. C. Loo and Q. Zhang, *Small*, 2015, **11**, 3440–3443.
127 J.-X. Feng, S.-Y. Tong, Y.-X. Tong and G.-R. Li, *J. Am. Chem. Soc.*, 2018, **140**, 5118–5126.
128 G. A. Snook, P. Kao and A. S. Best, *J. Power Sources*, 2011, **196**, 1–12.
129 S. K. D. Geetanjali and P. P. Kundu, *J. Power Sources*, 2022, **539**, 231595.
130 X. Liu, W. Wu and Z. Gu, *J. Power Sources*, 2015, **277**, 110–115.
131 L. A. Hernández, G. Riveros, D. M. González, M. Gacitua and M. A. del Valle, *J. Mater. Sci.: Mater. Electron.*, 2019, **30**, 12001–12011.
132 N. Senthilkumar, M. Pannipara, A. G. Al-Sehemi and G. Gnana kumar, *New J. Chem.*, 2019, **43**, 7743–7750.
133 S. Chen, S. A. Patil and U. Schröder, *Applied Energy*, 2018, **211**, 1089–1094.
134 W. Yang, Y. Peng, Y. Zhang, J. E. Lu, J. Li and S. Chen, *ACS Sustainable Chem. Eng.*, 2019, **7**, 3917–3924.
135 A. Anjum, S. A. Mazari, Z. Hashmi, A. S. Jatoi and R. Abro, *J. Electroanal. Chem.*, 2021, **899**, 115673.
136 M. Suermann, T. J. Schmidt and F. N. Büchi, *Electrochim. Acta*, 2018, **281**, 466–471.
137 S. Rojas-Carbonell, K. Artyushkova, A. Serov, C. Santoro, I. Matanovic and P. Atanassov, *ACS Catal.*, 2018, **8**, 3041–3053.
138 W. P. Mounfield, A. Garg, Y. Shao-Horn and Y. Román-Leshkov, *Chem*, 2018, **4**, 18–19.
139 H. Yuan, Y. Hou, I. M. Abu-Reesh, J. Chen and Z. He, *Mater. Horiz.*, 2016, **3**, 382–401.
140 J. Y. Chen, P. Xie and Z. P. Zhang, *Chem. Eng. J.*, 2019, **361**, 615–624.
141 B. Koo, S.-M. Lee, S.-E. Oh, E. J. Kim, Y. Hwang, D. Seo, J. Y. Kim, Y. H. Kahng, Y. W. Lee, S.-Y. Chung, S.-J. Kim, J. H. Park and S. P. Jung, *Electrochim. Acta*, 2019, **297**, 613–622.
142 X. Tian, M. Zhou, M. Li, C. Tan, L. Liang and P. Su, *Fuel*, 2018, **223**, 422–430.
143 G. P. Salvador, M. Gerosa, A. Sacco, N. Garino, M. Castellino, G. Massaglia, L. Delmondo, V. Agostino, V. Margaria, A. Chiodoni and M. Quaglio, *Energy Technol.*, 2018, **6**, 1052–1059.
144 X. Tian, M. Zhou, C. Tan, M. Li, L. Liang, K. Li and P. Su, *Chem. Eng. J.*, 2018, **348**, 775–785.
145 Y.-J. Choi, H. O. Mohamed, S.-G. Park, R. B. A. Mayyahi, M. Al-Dhaifallah, H. Rezk, X. Ren, H. Yu and K.-J. Chae, *Int. J. Hydrogen Energy*, 2020, **45**, 5960–5970.
146 Md. T. Noori, B. R. Tiwari, M. M. Ghangrekar and B. Min, *Sustainable Energy Fuels*, 2019, **3**, 3430–3440.
147 J. Chen, Y. Liu, J. Yang, H. Wang, H. Liu, S. Cao, X. Zhang, R. Wang, Y. Liu and Y. Yang, *Bioresour. Technol.*, 2022, **346**, 126584.
148 L. Jiang, J. Chen, D. Han, S. Chang, R. Yang, Y. An, Y. Liu and F. Chen, *J. Power Sources*, 2020, **453**, 227877.
149 M. Kodali, S. Herrera, S. Kabir, A. Serov, C. Santoro, I. Ieropoulos and P. Atanassov, *Electrochim. Acta*, 2018, **265**, 56–64.
150 Y. Wang, K. Zhong, H. Li, Y. Dai, H. Zhang, J. Zuo, J. Yan, T. Xiao, X. Liu, Y. Lu, M. Su and J. Tang, *J. Power Sources*, 2021, **485**, 229273.
151 S. Xin, J. Shen, G. Liu, Q. Chen, Z. Xiao, G. Zhang and Y. Xin, *Chem. Eng. J.*, 2020, **380**, 122446.
152 W. Yang, G. Chata, Y. Zhang, Y. Peng, J. E. Lu, N. Wang, R. Mercado, J. Li and S. Chen, *Nano Energy*, 2019, **57**, 811–819.
153 G. Pasternak, J. Greenman and I. Ieropoulos, *Applied Energy*, 2016, **173**, 431–437.
154 G. Alemany-Molina, J. Quílez-Bermejo, M. Navlani-García, E. Morallón and D. Cazorla-Amorós, *Carbon*, 2022, **196**, 378–390.
155 X. Wang, H. Zhang, J. Ye and B. Li, *J. Power Sources*, 2023, **556**, 232434.
156 K. Huang, L. Zhang, T. Xu, H. Wei, R. Zhang, X. Zhang, B. Ge, M. Lei, J.-Y. Ma, L.-M. Liu and H. Wu, *Nat. Commun.*, 2019, **10**, 606.
157 B. Liang, X. Zhang, M. Zhong, C. Lv and K. Li, *J. Power Sources*, 2021, **506**, 230178.
158 B. Liang, Y. Zhao, M. Zong, S. Huo, I. U. Khan, K. Li and C. Lv, *Chem. Eng. J.*, 2020, **385**, 123861.
159 K. Namsheer and C. S. Rout, *RSC Adv.*, 2021, **11**, 5659–5697.

160 L. Benny Mattam, A. Bijoy, D. Abraham Thadathil, L. George and A. Varghese, *ChemistrySelect*, 2022, **7**, e202201765.
161 C. Li, L. Ding, H. Cui, L. Zhang, K. Xu and H. Ren, *Bioresour. Technol.*, 2012, **116**, 459–465.
162 J. Ahmed, H. J. Kim and S. Kim, *J. Electrochem. Soc.*, 2012, **159**, B497.
163 Y. Pang, D. Xie, B. Wu, Z. Lv, X. Zeng, C. Wei and C. Feng, *Synth. Met.*, 2013, **183**, 57–62.
164 M. Priyadarshini, A. Ahmad, S. Das and M. M. Ghangrekar, *Int. J. Environ. Sci. Technol.*, 2022, **19**, 11539–11560.
165 S. Li, X. Zhu, H. Yu, X. Wang, X. Liu, H. Yang, F. Li and Q. Zhou, *Environ. Res.*, 2021, **197**, 111054.
166 R. Rossi, W. Yang, L. Setti and B. E. Logan, *Bioresour. Technol.*, 2017, **233**, 399–405.
167 P. Mukherjee and P. Saravanan, *J. Environ. Chem. Eng.*, 2022, **10**, 108940.
168 P. Mukherjee, U. Sharma and P. Saravanan, *Int. J. Energy Res.*, 2022, **46**, 23326–23340.
169 H. Zhang, Y. Wang, T. Wu, J. Yu, S. R. B. Arulmani, W. Chen, L. Huang, M. Su, J. Yan and X. Liu, *J. Alloys Compd.*, 2023, **944**, 169039.
170 H. Liu and B. E. Logan, *Environ. Sci. Technol.*, 2004, **38**, 4040–4046.
171 A. de Rosset, P. Rutkowski and G. Pasternak, *Sustain. Energy Technol. Assess.*, 2023, **58**, 103340.
172 J. Ahmed, H. J. Kim and S. Kim, *J. Electrochem. Soc.*, 2012, **159**, B497.
173 M. Rahimnejad, M. Ghasemi, G. Najafpour, M. Ismail, A. Mohammad, A. Ghoreyshi and S. H. Hassan, *Electrochim. Acta*, 2012, **85**, 700–706.
174 M. Behera, P. S. Jana and M. Ghangrekar, *Bioresour. Technol.*, 2010, **101**, 1183–1189.
175 D. A. Jadhav, S.-G. Park, T. Eisa, A. K. Mungray, E. C. Madenli, A.-G. Olabi, M. A. Abdelkareem and K.-J. Chae, *Renewable Sustainable Energy Rev.*, 2022, **167**, 112769.
176 G. Pasternak, J. Greenman and I. Ieropoulos, *ChemSusChem*, 2016, **9**, 88–96.
177 M. Shabani, H. Younesi, M. Pontié, A. Rahimpour, M. Rahimnejad and A. A. Zinatizadeh, *J. Cleaner Prod.*, 2020, **264**, 121446.
178 S. Anappara, K. Senthilkumar and H. Krishnan, in *Nanotechnology in Fuel Cells*, Elsevier, 2022, pp. 261–284.
179 K. J. Chae, M. Choi, F. F. Ajayi, W. Park, I. S. Chang and I. S. Kim, *Energy Fuels*, 2008, **22**, 169–176.
180 D. J. Kim, M. J. Jo and S. Y. Nam, *J. Ind. Eng. Chem.*, 2015, **21**, 36–52.
181 M. Ghasemi, S. Shahgaldi, M. Ismail, Z. Yaakob and W. R. W. Daud, *Chem. Eng. J.*, 2012, **184**, 82–89.
182 H. Yusuf, M. S. M. Annuar, S. M. D. Syed Mohamed and R. Subramaniam, *Chem. Eng. Commun.*, 2019, **206**, 731–745.
183 P. Narayanaswamy Venkatesan and S. Dharmalingam, *J. Membr. Sci.*, 2013, **435**, 92–98.
184 D. Vidhyeswari, A. Surendhar and S. Bhuvaneshwari, *Chemosphere*, 2022, **293**, 133560.
185 M. Rahimnejad, M. Ghasemi, G. D. Najafpour, M. Ismail, A. W. Mohammad, A. A. Ghoreyshi and S. H. A. Hassan, *Electrochim. Acta*, 2012, **85**, 700–706.
186 K. Ben Liew, J. X. Leong, W. R. Wan Daud, A. Ahmad, J. J. Hwang and W. Wu, *J. Power Sources*, 2020, **449**, 227490.
187 M. Sugumar, V. Kugarajah and S. Dharmalingam, *Process Saf. Environ. Prot.*, 2022, **158**, 474–485.
188 L. Di Palma, I. Bavasso, F. Sarasini, J. Tirillò, D. Puglia, F. Dominici and L. Torre, *Eur. Polym. J.*, 2018, **99**, 222–229.
189 A. K. M. Ali, M. E. A. Ali, A. A. Younes, M. M. Abo El fadl and A. B. Farag, *J. Hazard. Mater.*, 2021, **419**, 126420.
190 S. Shahgaldi, M. Ghasemi, W. R. Wan Daud, Z. Yaakob, M. Sedighi, J. Alam and A. F. Ismail, *Fuel Process. Technol.*, 2014, **124**, 290–295.
191 A. A. Olayiwola Sirajudeen, M. S. Mohamad Annuar, K. A. Ishak, H. Yusuf and R. Subramaniam, *J. Cleaner Prod.*, 2021, **278**, 123449.
192 H.-Y. Jung and S.-H. Roh, *J. Nanosci. Nanotechnol.*, 2020, **20**, 5711–5715.
193 L. Souza, R. Antônio, D. Hotza, C. Carminatti, T. Pineda-Vásquez, E. Watzko, A. P. Pezzin, D. Duarte and D. Recouvreux, *Mater. Chem. Phys.*, 2023, **293**, 126963.
194 M. M. Hasani-Sadrabadi, E. Dashtimoghadam, S. N. Saeedi Eslami, G. Bahlakeh, M. A. Shokrgozar and K. I. Jacob, *Polymer*, 2014, **55**, 6102–6109.
195 N. Saniei, N. Ghasemi, A. A. Zinatizadeh, S. Zinadini, M. Ramezani and A. A. Derakhshan, *Environ. Technol. Innovation*, 2022, **25**, 102168.
196 A. Sivasankaran and D. Sangeetha, *Fuel*, 2015, **159**, 689–696.
197 Y. Zhang, in *Nanotechnology in Fuel Cells*, Elsevier, 2022, pp. 285–347.
198 M. Mashkour, M. Rahimnejad, F. Raouf and N. Navidjouy, *Biofuel Res. J.*, 2021, **8**, 1400–1416.
199 R. Ding, S. Zhang, Y. Chen, Z. Rui, K. Hua, Y. Wu, X. Li, X. Duan, X. Wang and J. Li, *Energy*, 2022, 100170.
200 A. Alabi, A. AlHajaj, L. Cseri, G. Szekely, P. Budd and L. Zou, *npj Clean Water*, 2018, **1**, 10.
201 S. Mohsenpour, A. Kamgar and F. Esmaeilzadeh, *J. Inorg. Organomet. Polym. Mater.*, 2018, **28**, 63–72.
202 V. Kugarajah and S. Dharmalingam, *Chem. Eng. J.*, 2020, **398**, 125558.
203 Q. Liu, Z. Li, D. Wang, Z. Li, X. Peng, C. Liu and P. Zheng, *Front. Chem.*, 2020, **8**, 694.
204 S. Hosseini, S. Madaeni, A. Khodabakhshi and A. Zendehnam, *J. Membr. Sci.*, 2010, **365**, 438–446.
205 V. Kugarajah and S. Dharmalingam, *Chem. Eng. J.*, 2021, **415**, 128961.

